International Journal of Engineering and Technology Innovation, vol. 13, no. 1, 2023, pp. 14-27

A Robust Technique for Detection, Diagnosis, and Localization of Switching Faults in Electric Drives Using Discrete Wavelet Transform

Hari Kumar Raveendran Pillai*, Mayadevi Nanappan, Mini Valiyakulam Prabhakaran, Shenil Pushpangadan Sathyabhama

Department of Electrical Engineering, College of Engineering Trivandrum, Kerala, India

Received 17May 2022; received in revised form 14July 2022; accepted 17July 2022

DOI: https://doi.org/10.46604/ijeti.2023.10005

Abstract

Detection, diagnosis, and localization of switching faults in electric drives are extremely important for operating a large number of induction motors in parallel. This study aims to present the design and development of switching fault detection, diagnosis, and localization strategy for the induction motor drive system (IMDS) by using a novel diagnostic variable that is derived from discrete wavelet transform (DWT) coefficients. The distinctiveness of the proposed algorithm is that it can identify single/multiple switch open and short faults and locate the defective switches using a single mathematical computation. The proposed algorithm is tested by simulation in MATLAB/Simulink and experimentally validated using the LabVIEW hardware-in-the-loop platform. The results demonstrate the robustness and effectiveness of the proposed technique in identifying and locating faults.

Keywords: induction motor, electric drives, discrete wavelet transform, switch open faults, switch short faults

1. Introduction

Induction motors (IMs) have found widespread applications in industries with harsh and contaminated work environments due to their rugged construction, ease of design and maintenance, high power-to-weight ratio, and low cost-to-power ratio. The variable speed operation of these motors is enabled by using variable frequency AC drives.

However, the use of power electronic devices in the drive makes the induction motor drive system (IMDS) susceptible to diverse faults. The detection and diagnosis of these faults in IMDS are critical to industries to avoid unforeseen production shutdowns that lead to financial losses. Therefore, to ensure the profitability of any industry, together with fault preventative measures, an accurate fault detection, diagnosis, and localization system supported by non-invasive condition monitoring is necessary.

The origination of faults in the IMDS is generally manifested by the fluctuations in the motor's operating parameters such as stator current, voltage, electromagnetic field, etc. Hence, precise fault detection and localization can be accomplished by a sensible review of the trends and variations in stator current, voltage, and electromagnetic field. Various techniques have been presented in the literature for detecting, localizing, and isolating faults in electric drives [1-3].

The diagnosis of open circuit (OC) in power devices is highly desirable since they frequently result in serious secondary faults. Park's vector-based technique is utilized for switch open (SO) fault detection [4]. This method is load-dependent; moreover, due to the requirement for composite pattern recognition, the technique is complex and less robust. The

* Corresponding author. E-mail address: harikumar@cet.ac.in

Tel.: +91-471-2515838; Fax: +91-471-2515502

second-order rotational Park transformation-based technique is used for SO fault detection in IMDS [5]. This method is computationally intensive and has a limitation in handling noisy signals. Shi et al. [6] utilized a moving integration filter. The error between the predicted and estimated values of the current signal is used for SO fault diagnosis. However, after a fault, the control loop provides inaccurate features as it cannot track the reference.

Hu et al. [7] reconstructed the phase voltages and derived the residual behaviors for faulty conditions using a switching function to detect the SO fault. This strategy does not work well under low-speed conditions. The *dq*-axis current residuals are utilized in [8] to detect SO faults in the permanent magnet synchronous motor (PMSM) drive system. The discrepancy between the predicted and the estimated fluxes are used for detecting SO faults [9]. Artificial intelligence-based techniques are also widely used for fault detection, such as neural networks [10], support vector machines [11], fuzzy logic [12], hybrid techniques such as wavelet neural networks [13], and multi-sensory control with wavelet analysis [14].

However, these techniques are computationally intensive and less robust. Recent progress in the domain of multiple SO fault diagnosis reports the use of either variation of existing methods or a combination of proven algorithms. The detection and timely isolation of a switch short (SS) fault in the inverter of IMDS are very critical as high currents severely damage the system. Short circuit (SC) fault analysis schemes, in general, rely on monitoring various parameters such as voltage, stator current, gate current, motor speed, and torque.

Masrur et al. [15] presented a single strategy capable of detecting and diagnosing SO and SS faults based on an artificial neural network. Extensive training requirements are a major drawback while implementing the system for industry-based applications. Gameiro and Marques Cardoso [16] proposed an approach that employed an extra current sensor for measuring current in the DC-link. An algorithm based on the deviation of average current with respect to the reference current is used for SO and SS fault diagnosis [17]. However, the algorithm is applicable only for drives with closed-loop control systems.

Mayadevi et al. [18] presented a fuzzy-based algorithm for the detection and diagnosis of drive faults in IMDS. It uses the root mean square (RMS) value of stator currents, and its total harmonic distortion (THD) during the fault. Ali et al. [19] used a machine learning-based fault diagnosis which is based on matching pursuit and DWT of stator currents and vibration signals. Zaman and Liang [20] used graph-based semi-supervised learning for fault diagnosis of IMs.

Shao et al. [21] presented a deep learning-based multi-signal fault diagnosis of IMs utilizing the wavelet transform of the sensor signals. Abbasi and Mahmoudi [22] presented a statistical control charts-based technique to discriminate faults in electrical machines. Abbasi [23] presented a comprehensive review that identified various parameters to be considered during the design and development of fault diagnosis techniques for electrical equipment.

The research on fault diagnosis of IMDS is diverse. However, the need to develop a generalized solution competent in detecting both SO and SS faults using a single mathematical computation at variable load conditions is noted. Therefore, this study employs an effective and comprehensive fault diagnosis approach for detecting and localizing both SO and SS faults. The approach is based on the DWT of the three-phase stator currents alone. The main contributions of this study include the following:

- A fault diagnosis method using a novel diagnostic variable, the 10^{th} level aggregate wavelet coefficient (C_{10}), to detect and localize both SO and SS faults.
- A simple approach that requires only a single-step computation.
- A robust technique for SO and SS fault detection and localization, independent of variations in load, speed, and parameter value.
- Performance validated in hardware.

2. Faults in IMDS

IMDS comprises an ac voltage source, a rectifier for converting the AC to DC voltage, a DC-link capacitor, an inverter, and an induction motor (IM). The possible switching faults in IMDSs are illustrated in Fig. 1. They are SC of rectifier diode (F1), OC of rectifier diode (F2), DC-link capacitor getting short-circuited (F3) or earthed (F4), SC of inverter switch (F5), and OC of inverter switch (F6) [24]. Faults occur at F5 and F6 most commonly.

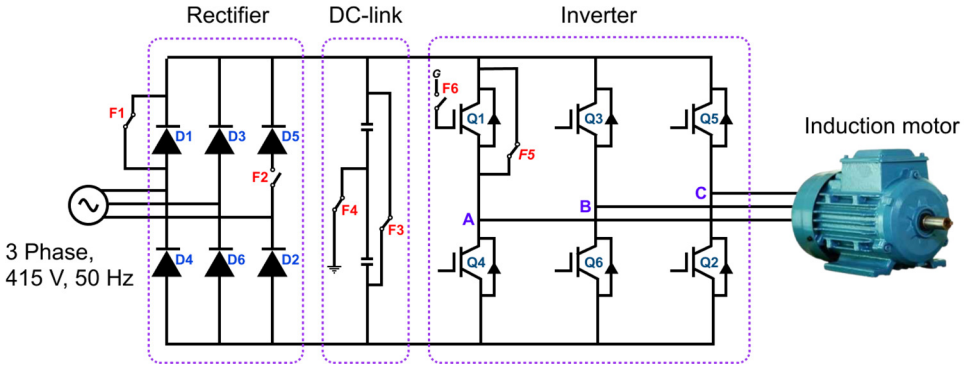

Fig. 1 Schematic representation of faults in IMDS

2.1. Fault simulation

In this study, the parameters of a three-phase, 1 hp, 400 V, 50 Hz, and 1440 rpm squirrel cage IM are acquired from the virtual model designed in ANSYS RMxprt. The parameters extracted are as follows: stator resistance (R_s) = 10.592 Ω, rotor resistance (R_r) = 34.5673 Ω, core loss component (R_c) = 11269 Ω, stator leakage reactance (X_{Ls}) = 12.7611 Ω, rotor leakage reactance (X_{Lr}) = 8.96771 Ω, and a magnetizing reactance (X_{Lm}) = 143.471 Ω. Using these parameters, the IM is modeled in MATLAB/Simulink. To analyze IMDS performance, the load is applied at 2 sec after starting the IMDS under no load. The SO and SS faults in IMDS are analyzed by creating a fault in the drive at 2.5 sec, using a breaker switch arrangement.

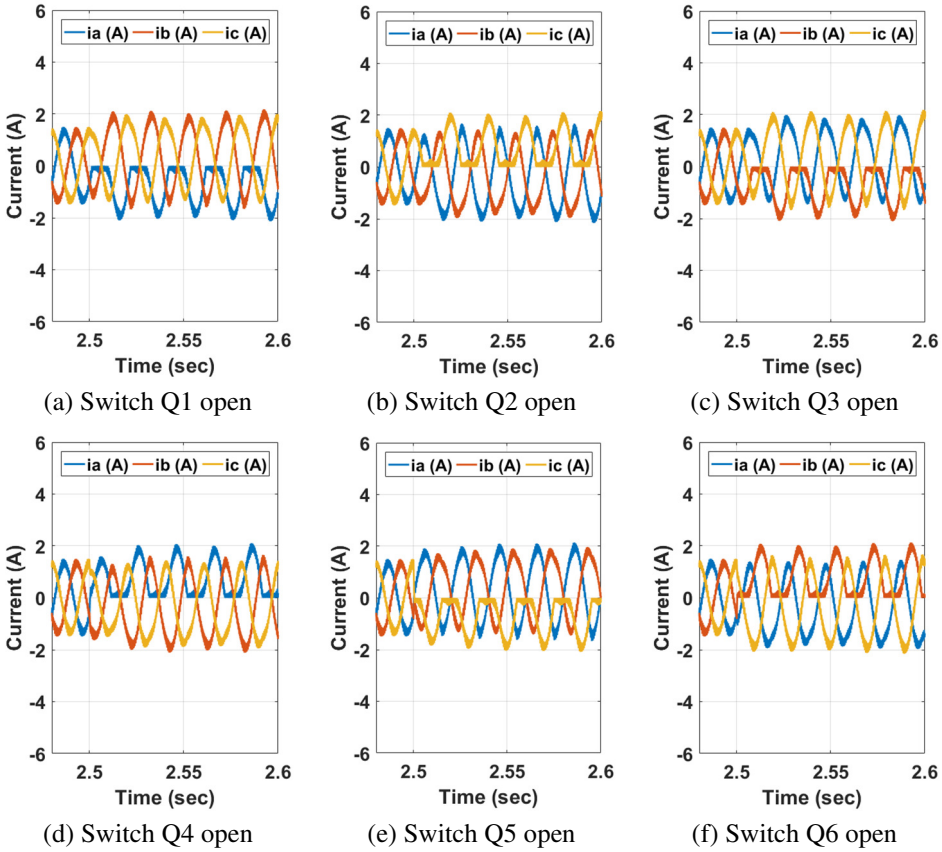

(a) Switch Q1 open (b) Switch Q2 open (c) Switch Q3 open

(d) Switch Q4 open (e) Switch Q5 open (f) Switch Q6 open

Fig. 2 Stator currents of IMDS with full load under SSO fault(continued)

As a first case, the single switch open (SSO) fault is created in IGBT "Q_1" of the inverter in IMDS. During a fault, the stator current in phase "*a*" contains AC values and DC offset values. Due to the symmetry of the phases, the phase "*a*" DC offset current will be equally distributed between phases "*b*" and "*c*". All individual switches are similarly analyzed and the current responses under full load are shown in Fig. 2. Furthermore, the double switch open (DSO) fault analysis is performed for all combinations of the fault. The current responses are portrayed in Fig. 3.

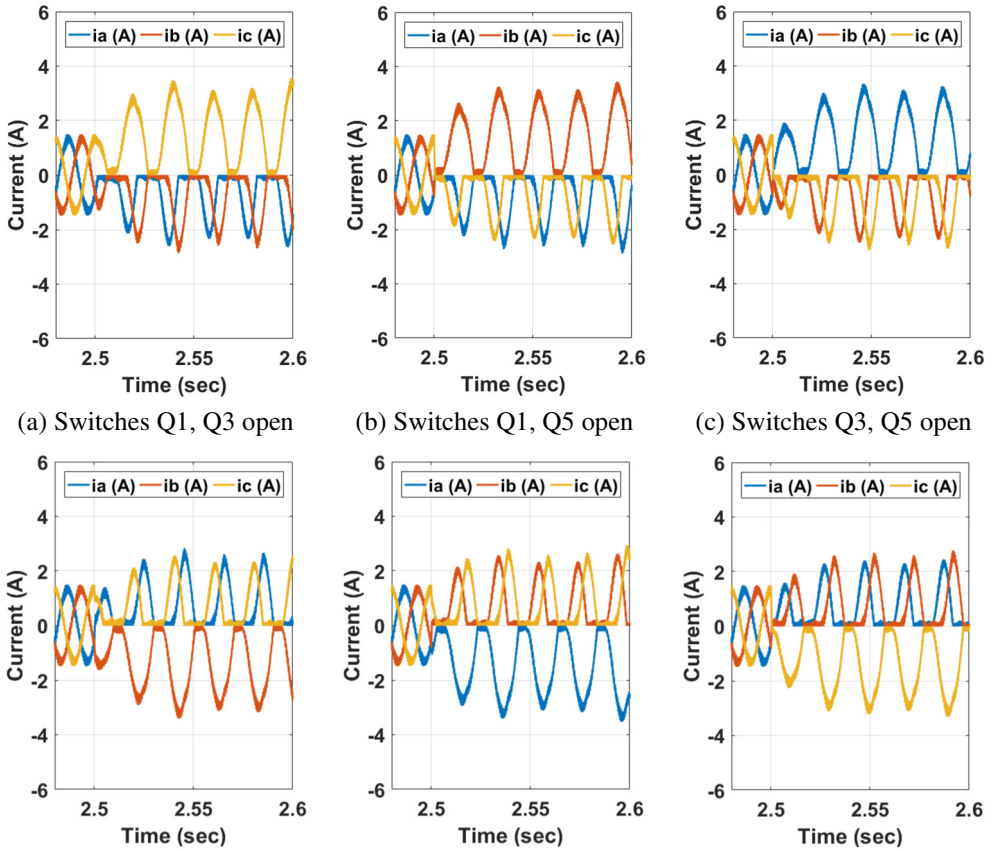

(a) Switches Q1, Q3 open (b) Switches Q1, Q5 open (c) Switches Q3, Q5 open

(d) Switches Q2, Q4 open (e) Switches Q2, Q6 open (f) Switches Q4, Q6 open

Fig. 3 Stator currents of IMDS with full load under DSO fault

The SS fault is analyzed in this work using a breaker switch arrangement to short the inverter IGBT. When IGBT "Q_1" is short, phase "*a*" is directly tied to the positive side of the DC-link, and phases "*b*" and "*c*" are unaltered. All single switch short (SSS) conditions are similarly analyzed, and the current responses under full load are shown in Fig. 4. The detailed analysis of the responses indicates that the fault suddenly deforms the current waveforms. It can be effectively apprehended using signal analysis techniques such as wavelet transform.

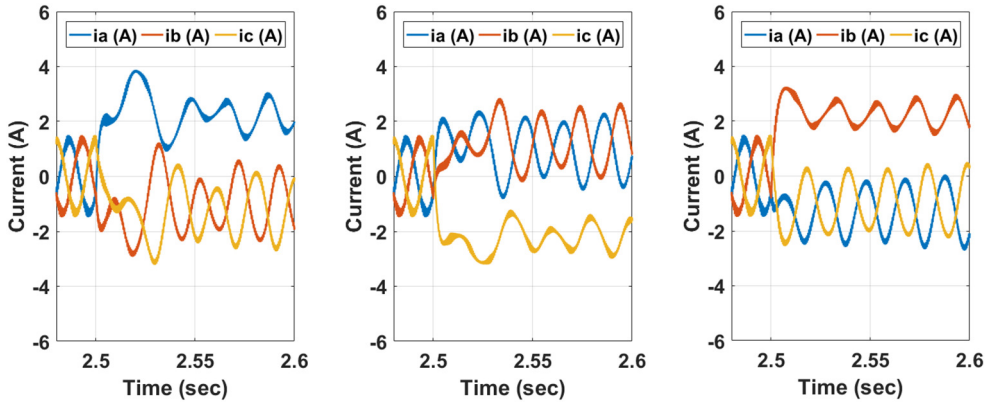

(a) Switch Q1 short (b) Switch Q2 short (c) Switch Q3 short

Fig. 4 Stator currents of IMDS with full load under SS fault

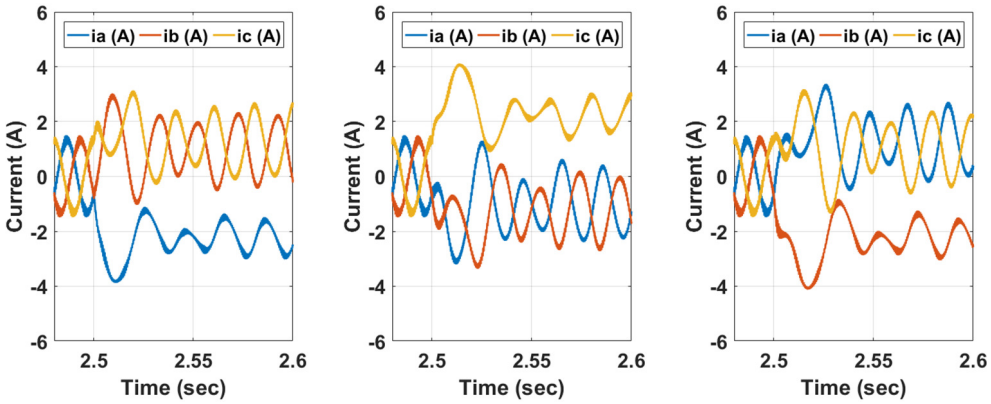

(d) Switch Q4 short (e) Switch Q5 short (f) Switch Q6 short

Fig. 4 Stator currents of IMDS with full load under SS fault (continued)

2.2. *Wavelet analysis*

Wavelet analysis is a persuasive tool developed to scrutinize rapidly changing transient signals and is widely used for signal and image processing applications. In the analysis, the signal is characterized by the sum of approximation and detail coefficients. Each set of coefficients is commensurate to a certain band of frequency [25].

The wavelet analysis offers insight into the different aspects of signals, such as trends, discontinuities, self-similarity, etc., by splitting the signal into scaled and shifted versions of the mother wavelet. The two basic classes of wavelet transform available for analysis are continuous wavelet transform and DWT. Robustness, excellent sensitivity, and short detection time make the multilevel DWT technique more ideal for online fault detection. Unlike Fourier and cosine transforms, the DWT has the advantage of being well represented and discretized in both time and frequency domains. This allows it to keep the time information intact [26].

2.3. *Fault detection and diagnosis using DWT*

To detect the SO and SS faults, the stator currents obtained with varying loads are decomposed using the multilevel DWT when IMDS is operating under normal and faulty conditions. The minimum number of decomposition levels (N) in the wavelet analysis is related to the sampling frequency (f_s) of the signal being analyzed and is represented by Eq. (1) [27]. This number allows the high-order signals resulting from the analysis to reflect the evolution of the signal components within the band 0-f Hz.

$$N > \frac{\log\left(\frac{f_s}{f}\right)}{\log 2} + 1, \text{ (integer)} \tag{1}$$

In this work, the frequency of the source is 50 Hz, and the switching frequency (f_s) is 10 kHz. Hence, the 10^{th} level of DWT is identified as optimal for the study. Through exhaustive analysis, a novel diagnostic variable, the 10^{th} level aggregate wavelet coefficient (C_{10}) is identified for the classification of faults. This variable is the average of the absolute values of wavelet coefficients of stator currents.

2.4. *Selection of the threshold values of C_{10}*

In this study, the IMDS of different capacities under varying loads and IM parameters are analyzed in detail to select the threshold value of the diagnostic variable C_{10} under SO and SS conditions. The C_{10} values computed with 1 hp IM under SO and SS faults, with 1/3 full load (FL), 2/3 FL, and FL are listed in Table 1. Under normal operating conditions with different loads, C_{10} is below 2. During the SO fault, C_{10} is in the range of 2-10, and above 10 during the SS fault. This inference forms

the basis for the design of the fault detection and localization algorithm. For generalization of the proposed technique, 5 hp IMDS is also analyzed in detail, and the C_{10} values are tabulated in Table 2. From Table 2, the C_{10} range for 5 hp IMDS is also discerned to be within the range selected for the 1 hp IMDS. Hence, it is concluded that if the stator currents are normalized, the selected C_{10} range can detect and diagnose faults in IMDS with varying capacities.

Table 1 C_{10} values obtained under fault in IMDS with 1 hp IM

Faulty switches	Aggregate wavelet coefficients					
	SO fault			SS fault		
	1/3 FL	2/3 FL	FL	1/3 FL	2/3 FL	FL
Q_1	6.03	6.38	6.56	11.30	12.6	13.81
Q_2	4.50	4.63	5.01	11.70	13.10	14.20
Q_3	5.23	5.40	5.50	12.41	13.70	14.20
Q_4	4.83	5.03	5.40	12.84	13.5	14.81
Q_5	5.89	5.95	5.98	12.66	13.1	14.77
Q_6	4.76	4.79	4.82	11.99	12.82	13.87
Q_1-Q_3	9.34	9.56	9.72	12.10	11.806	11.50
Q_1-Q_5	9.54	9.55	9.73	14.50	11.20	12.10
Q_3-Q_5	8.40	8.51	8.77	11.50	11.20	12.10
Q_2-Q_4	8.72	8.72	9.20	12.00	13.10	13.30
Q_2-Q_6	9.80	9.82	9.83	11.50	12.00	12.10
Q_4-Q_6	8.82	9.29	9.56	11.80	10.90	10.70

Table 2 C_{10} values obtained under fault in IMDS with 5 hp IM

Faulty switches	SO fault				SS fault			
	1/4 FL	1/2 FL	3/4 FL	FL	1/4 FL	1/2 FL	3/4 FL	FL
Q_1	6.70	6.90	6.50	7.80	13.80	14.20	12.10	15.80
Q_2	8.70	8.40	8.20	7.90	15.80	16.00	16.20	16.00
Q_3	9.20	9.20	9.10	8.20	14.90	15.10	16.20	15.90
Q_4	8.20	8.30	7.90	8.60	12.90	13.60	11.90	17.10
Q_5	8.90	9.10	8.80	9.30	14.10	15.50	16.40	16.90
Q_6	7.10	7.30	6.80	7.20	14.60	15.90	15.90	16.10
Q_1-Q_3	4.10	4.90	6.10	5.40	13.90	14.10	13.80	13.90
Q_1-Q_5	5.10	5.70	4.80	5.00	12.50	16.10	15.70	14.90
Q_3-Q_5	3.80	5.00	6.20	5.50	12.10	13.00	12.30	11.90
Q_2-Q_4	6.20	6.10	5.80	5.70	13.10	11.90	12.30	12.90
Q_2-Q_6	5.40	6.40	6.80	5.90	14.10	13.80	15.10	12.90
Q_4-Q_6	5.10	7.10	6.30	5.70	13.00	13.50	12.90	13.10

Table 3 C_{10} values obtained under SO fault in IMDS with 20% parameter variation in 1 hp IM

Faulty switches	SO fault			SS fault		
	Variation in R_s	Variation in L_s	Variation in R_s&L_s	Variation in R_s	Variation in L_s	Variation in R_s&L_s
Q_1	5.13	5.50	5.30	18.40	19.10	18.10
Q_2	4.20	4.90	4.80	19.10	19.50	18.90
Q_3	5.00	5.70	5.34	19.00	18.90	18.40
Q_4	5.30	5.60	5.10	19.10	19.70	19.50
Q_5	5.40	6.10	5.70	19.20	20.10	19.80
Q_6	3.80	4.30	3.90	17.30	18.50	17.90
Q_1-Q_3	8.70	9.10	8.85	12.70	13.70	12.40
Q_1-Q_5	7.85	8.10	7.85	17.20	17.50	16.80
Q_3-Q_5	7.10	6.90	7.60	15.90	16.10	15.80
Q_2-Q_4	7.15	6.80	7.65	16.90	17.50	17.20
Q_2-Q_6	8.70	9.10	8.80	14	14.30	13.80
Q_4-Q_6	8.20	7.80	8.90	14.90	15.40	14.70

To check the sensitivity of C_{10} to parameter variations, 1 hp IM has been analyzed under SO and SS faults with 20% variation in R_s alone, stator leakage inductance (L_s) alone, and both R_s & L_s together. The results are tabulated in Table 3. From Table 3, the values of C_{10} are evidently within the selected limits under all cases of SO and SS fault.

2.5. Faulty switch localization

A major issue to be addressed in fault localization is the identification of faulty switches in the inverter. Even though C_{10} can precisely diagnose the fault, additional diagnostic variables are necessary for fault localization. The faulty switch localization is accomplished using combinational values of diagnostic variables $C_P(I_a)$, $C_P(I_b)$, and $C_P(I_c)$ obtained using Eq. (2). These variables are the polarity of the post-fault 10th level coefficient of the stator currents in phases "*a*", "*b*", and "*c*", respectively. The values of the diagnostic variable for fault localization under single SO and SS faults are listed in Table 4.

$$C_p(I_k) = \begin{cases} \text{POS}, & C_{10} \geq 0 \\ \text{NEG}, & C_{10} < 0 \end{cases} \tag{2}$$

where k = a,b, and c are the three phases of the system.

Table 4 shows that if the diagnostic variable combination $C_P(I_{a,b,c})$ are "NEG, POS, POS" and the fault is SO, then IGBT "Q_1" is identified as open. Similarly, if $C_P(I_{a,b,c})$ are "NEG, POS, POS" and the fault diagnosed is SS, then, IGBT "Q_4" is identified as short. As the same value of $C_P(I_{a,b,c})$ yields different results, fault localization needs to be performed after its diagnosis.

Table 4 Diagnostic variables for fault localization

Faulty switch	SO fault			SS fault		
	$C_P(I_a)$	$C_P(I_b)$	$C_P(I_c)$	$C_P(I_a)$	$C_P(I_b)$	$C_P(I_c)$
Q_1	NEG	POS	POS	POS	NEG	NEG
Q_2	NEG	NEG	POS	POS	POS	NEG
Q_3	POS	NEG	POS	NEG	POS	NEG
Q_4	POS	NEG	NEG	NEG	POS	POS
Q_5	POS	POS	NEG	NEG	NEG	POS
Q_6	NEG	POS	NEG	POS	NEG	POS

3. Proposed Fault Diagnosis and Localization Algorithm

Fig. 5 and Fig. 6 depict the proposed algorithms for fault diagnosis and localization, respectively. The process begins with the continuous acquisition of IM stator currents I_a, I_b, and I_c. Then, it is normalized to make the fault diagnosis process independent of machine rating and operating conditions. Furthermore, the multilevel DWT decomposition is performed on the normalized currents to obtain the 10th level wavelet coefficients. C_{10} is computed by averaging the magnitude of the 10th level wavelet coefficients of all the phase currents. Under normal operating conditions, $0 \leq C_{10} < 2$. If a SO fault is detected ($2 \leq C_{10} \leq 10$), a variable "K" is set to "0", and if a SS fault is detected ($C_{10} > 10$), variable "K" is set to "1". After fault detection, the algorithm immediately switches off the system and advances to the fault localization algorithm to identify the faulty switch.

The fault localization algorithm uses the value of the stored diagnostic variables for identifying the faulty switch. As diagnostic variables have the same pattern for the SO and SS faults, the value of the "K" sets in the fault detection algorithm. Furthermore, the values of $C_p(I_{a,b,c})$ in Table 4 are used for identifying the faulty switch, e.g., if K = 0 and $C_p(I_{a,b,c})$ are "NEG, POS, POS," the IGBT "Q_4" is identified as open. If K = 1 and the $C_p(I_{a,b,c})$ are "NEG, POS, POS," the IGBT "Q_1" is identified as short. This feature will enable the operator to easily localize the fault and take the necessary steps for faster maintenance and restoration.

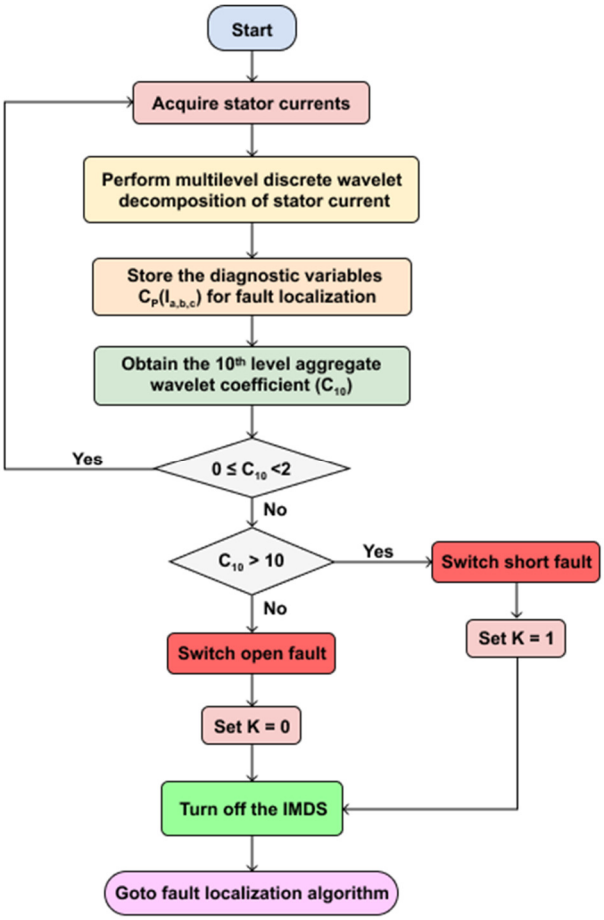

Fig. 5 Flowchart for fault diagnosis

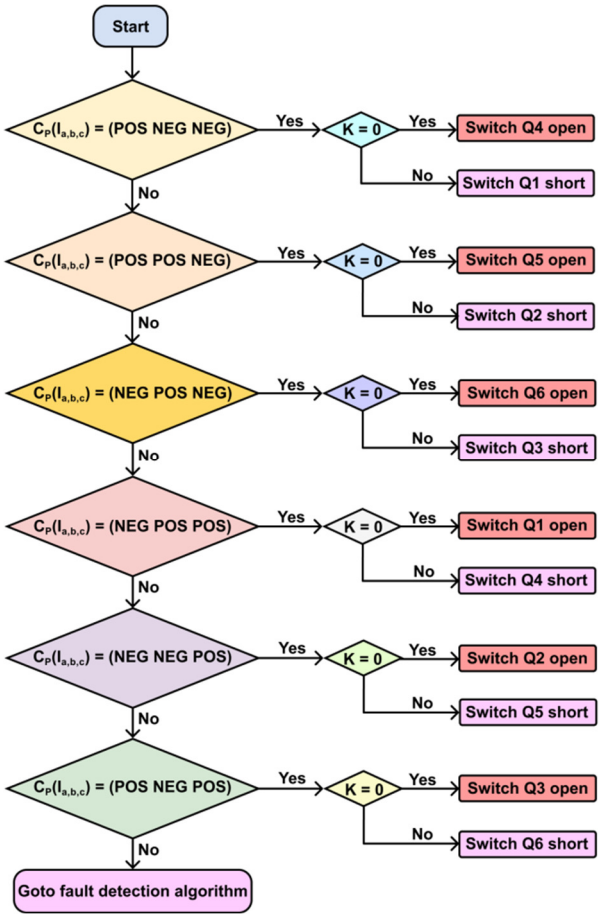

Fig. 6 Flowchart for fault localization

4. Testing of the Proposed Fault Detection and Localization Algorithm

The proposed algorithm is tested in IMDS with 1 hp IM, under varying operating conditions. The simulation results are put forward to manifest their feasibility under the SO and SS faults. Fig. 7 and Fig. 8 show the stator current waveforms of all three phases, the diagnostic variable, and the alarm signal under the SSO and DSO faults, respectively. The waveforms are recorded with a load of 2.5 Nm and the motor running at the rated speed. The IGBT "Q_3" is permanently forced open at 2.5 sec. From Fig.7, it can be seen that the alarm signal is triggered at 2.516 sec, i.e., less than one cycle. Similarly, when the IGBTs "Q_1" and "Q_3" are permanently forced open at 2.5 sec, the alarm signal is triggered at 2.516 sec as seen in Fig. 8.

Fig. 9 shows the stator current waveforms of all three phases, the diagnostic variable, and the alarm signal under SSS fault. The load is 2.5 Nm and the motor runs at the rated speed. As seen in Fig. 9, the alarm signal is triggered at 2.516 sec when the IGBT "Q_5" is permanently forced short at 2.5 sec.

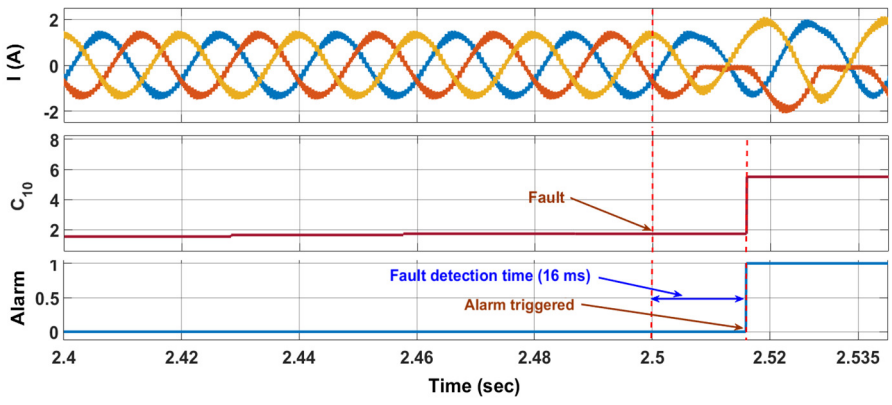

Fig. 7 Stator currents, diagnostic signal, and alarm signal under SSO fault

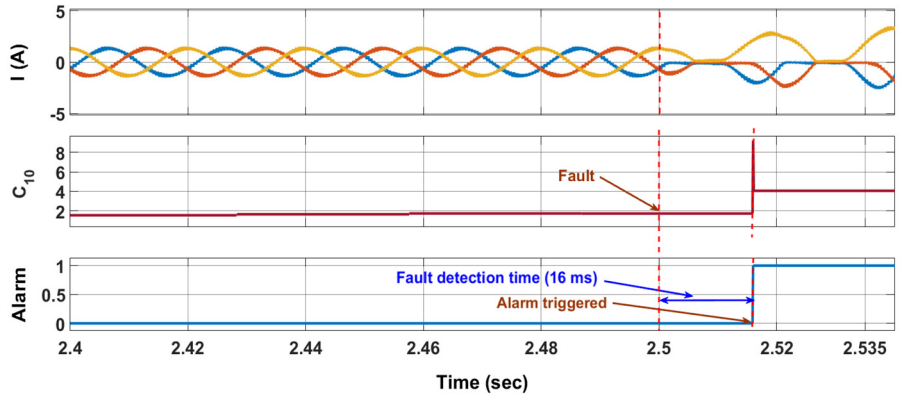

Fig. 8 Stator currents, diagnostic signal, and alarm signal under DSO fault

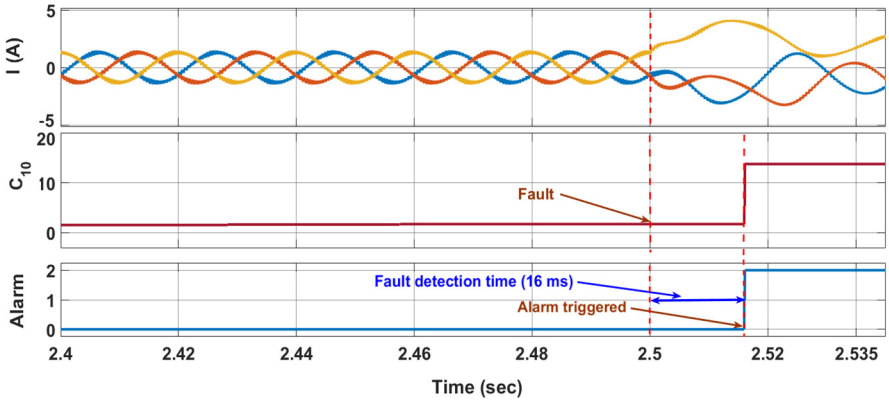

Fig. 9 Stator currents, diagnostic signal, and alarm signal under SSS fault

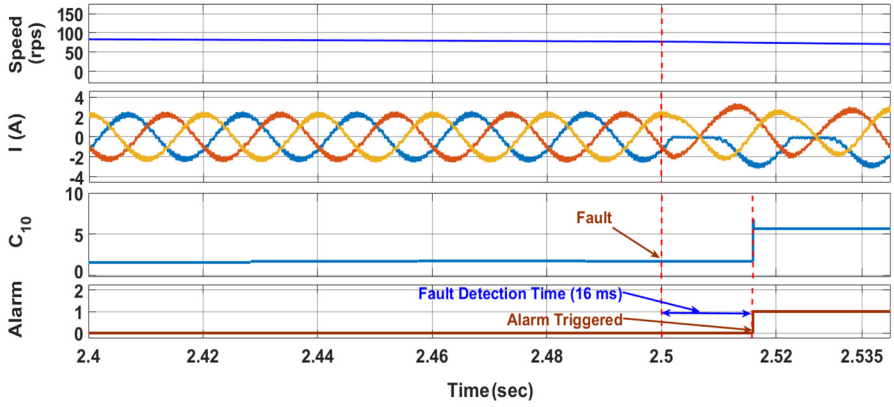

Fig. 10 Motor speed, stator currents, diagnostic signal, and alarm signal under SSO fault (operating at reduced speed)

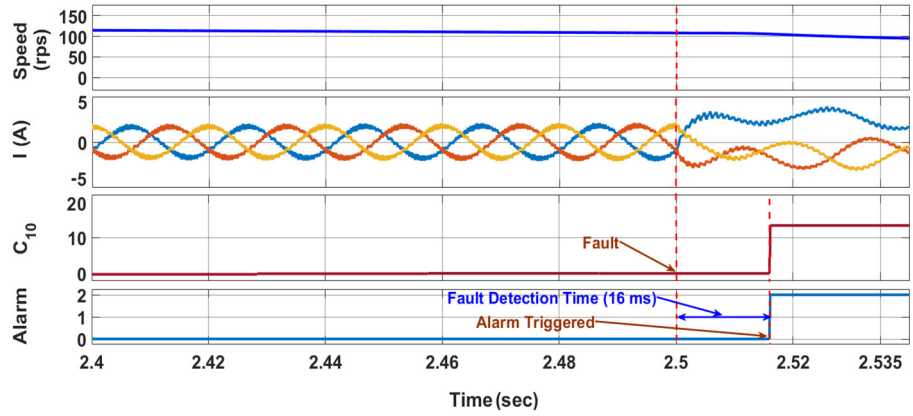

Fig. 11 Motor speed, stator currents, diagnostic signal, and alarm signal under SSS fault (operating at reduced speed)

Fig. 10 and Fig. 11 show the motor speed, stator current waveforms of all three phases, the diagnostic variable, and the alarm signal under SO and SS fault at speeds less than the rated value. In these cases, the faults were introduced at 2.5 sec. The alarm signal can be seen to be triggered at 2.516 sec, which is less than one cycle. Hence, the performance of the proposed algorithm can be ascertained to be unaffected by changes in the operating speed.

Fig. 12 and Fig. 13 show the stator current waveforms of all three phases, the diagnostic variable, and the alarm signal under the SO and SS faults, respectively, under load change. In both cases, a load change is introduced at 2.0 sec, and the fault was introduced at 2.5 sec. During the load change at 2.0 sec, the diagnostic variable value can be noted to remain within 2, and the alarm is not triggered. At 2.516 sec, the alarm signal is triggered due to the fault introduced at 2.5 sec. Hence, it can be noted that the proposed algorithm works well under transient conditions.

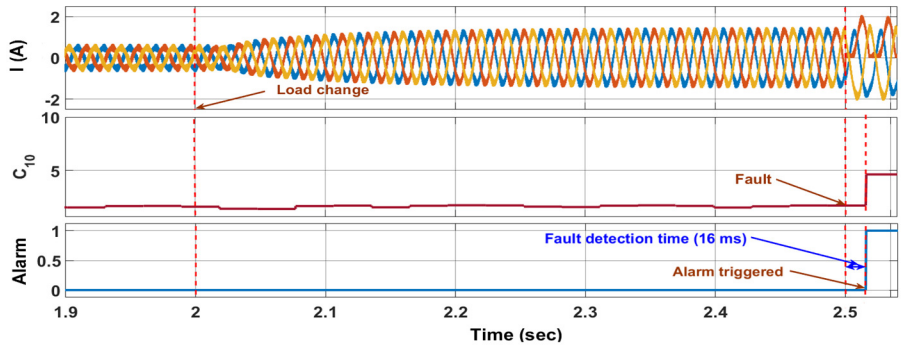

Fig. 12 Stator currents, diagnostic signal, and alarm signal during load change and SSO fault

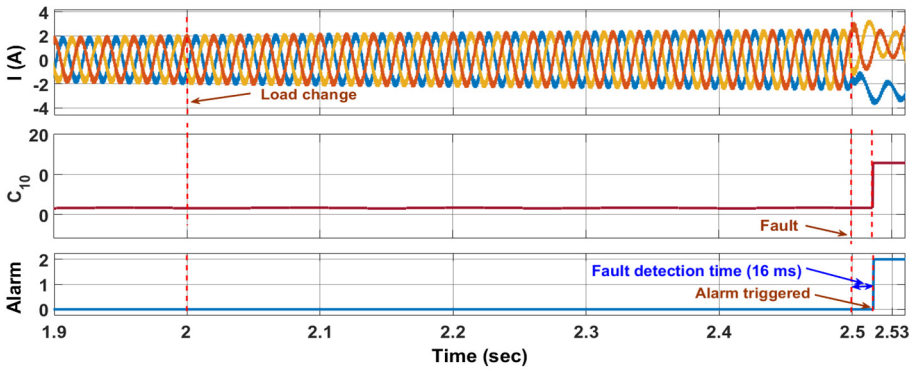

Fig. 13 Stator currents, diagnostic signal, and alarm signal during load change and SSS fault

5. Performance Comparison

In this section, the effectiveness of the proposed technique is justified by comparing it with various fault diagnosis techniques in the literature. The data are summarized in Table 5. The following list of evaluation indices is selected for comparison: the types of fault that can be detected, detection time, robustness (effect of load variation, speed variation, etc., on the performance of the algorithm), tuning effort (the number of thresholds and tolerances to be set), cost, sensitivity to parameter variation, and effort for implementation.

From Table 5, the proposed method can be seen to diagnose SSO, DSO, SSS, and double switch short (DSS) faults with a single algorithm. The detection and diagnosis time for the proposed algorithm is less than one cycle (16 ms). Moreover, the proposed technique is highly robust as it is independent of load variations and speed variations. This fact is evident from the results depicted in Figs. 10-13. Additionally, the tuning effort of the proposed fault diagnosis algorithm is less as it needs only a one-time setting of two threshold values for fault diagnosis (Normal: $C_{10} < 2$, SO fault (F5): $2 \leq C_{10} \leq 10$, and SS fault (F6): $C_{10} > 10$). The implementation effort and cost are less as it needs only two sensors and one field-programmable gate array (FPGA) board for deployment in the field.

Table 5 Performance comparison of the fault detection and diagnosis methods

Fault diagnosis method	Detection time	Robustness	Types of fault detected				Tuning effort	Cost	Sensitivity to parameter variation	Implementation
			SSO	DSO	SSS	DSS				
Park's vector [4]	< 2 cycles	Low	Yes	No	No	No	High	Low	Low	Simple
Second-order rotational Park transformation [5]	< 1/2 cycle	High	Yes	No	No	No	Medium	Low	Low	Simple
Moving integration filter-based [6]	Within one cycle	High	Yes	Yes	No	No	Medium	Low	Low	Simple
Phase voltage reconstruction and residual generation [7]	< 2cycles	Low	Yes	Yes	No	No	Medium	Low	High	Complex
Neural networks [13]	20 ms	High	Yes	Yes	Yes	Yes	High	High	High	Complex
Load current similarity analysis [28]	5 ms	High	Yes	Yes	No	No	Medium	Less	Low	Complex
Modified Park's vector method [29]	> 2 cycles	Low	Yes	No	No	No	High	Low	Low	Simple
Normalized DC current [29]	Less than one cycle	Low	Yes	No	No	No	Low	Low	Low	Simple
Current angle-based method [30]	5 ms	Low	Yes	No	No	No	Medium	Low	Low	Simple
Proposed method	**< 1 cycle (16 ms)**	**High**	**Yes**	**Yes**	**Yes**	**Yes**	**Low**	**Low**	**Very low**	**Simple**

6. Experimental Validation

The proposed fault detection and localization algorithm under SSO and DSO faults are experimentally validated on a three-phase IMDS. The scheme and the experimental setup are shown in Fig. 14 and Fig. 15, respectively. The IMDS consists of a three-phase, 1 hp, 415 V, 50 Hz IM fed from a Semikron make rectifier/inverter stack. The power switches used in the inverter are IGBTs (SKM75GB12T4).

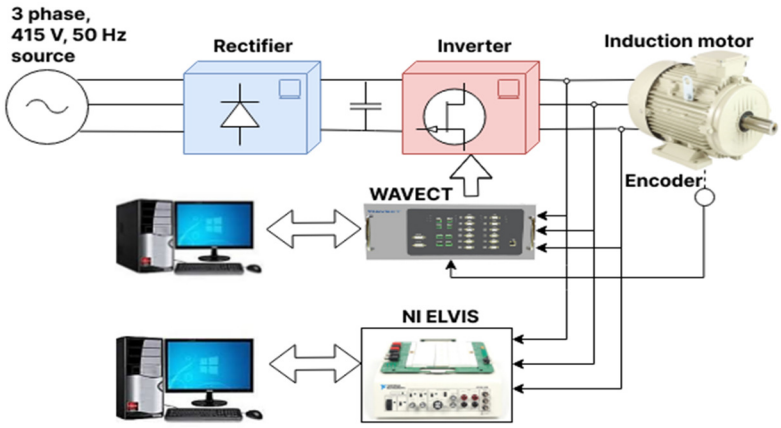

Fig. 14 Block diagram of the experimental setup for validation

The input to the three-phase inverter is from the diode bridge rectifier, which is fed from a three-phase 415 V, 50 Hz source. The DC-link of the rectifier/inverter stack ensures constant DC input voltage to the inverter. The 10 kHz PWM gate signals generated from WAVECT, a real-time control prototyping system, are provided through the gate drive of the inverter. The WAVECT has a high-end FPGA for fast computing, input and output ports, a dual-core processor for control and communication, and sensors for voltage and current measurements.

A data monitoring and diagnosis system consisting of LEM LA-50P current sensors, NI ELVIS data acquisition platform, and LabVIEW software are employed in this study. This system accurately acquires the stator currents of IM. The 16-bit A/D converters in the NI ELVIS, which have a maximum multi-channel sampling rate of 1.00 MSa/s, are used for sampling the

current signals. The acquired stator currents are filtered using a low pass filter and passed through the wavelet block in LabVIEW. The Daubechies 4 (db4) mother wavelet is used in this study for the analysis. Furthermore, the absolute value of the wavelet coefficients of the three phases is averaged to obtain the aggregate wavelet coefficient. This value is passed through the developed algorithm block that identifies the type of fault. The algorithm detects the fault and issues a warning message to the operator that the inverter switch is open at the instant of the SO condition.

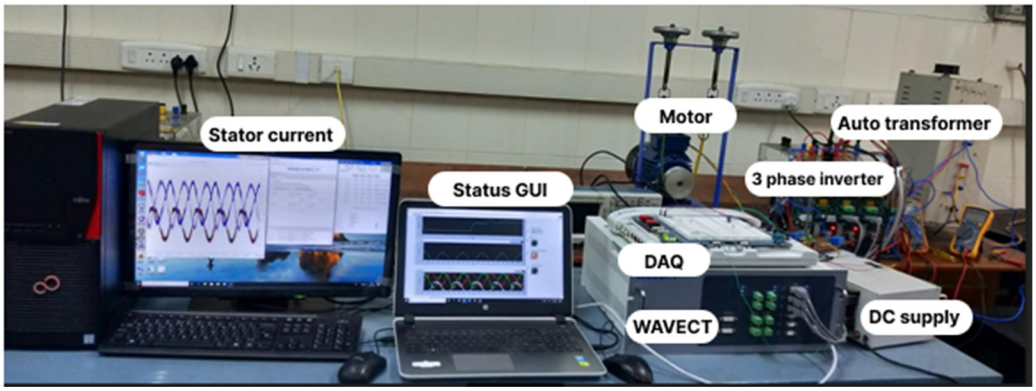

Fig. 15 Experimental setup of 1 hp IMDS for validation

The proposed algorithm is experimentally validated during SSO and DSO faults when operating under all load conditions to substantiate its effectiveness. The time-domain stator current waveforms and the corresponding diagnostic signal under a typical case of SSO and DSO fault obtained from LabVIEW are shown in Fig. 16 and Fig. 17, respectively. From the experimental results, under normal operating conditions the C_{10} value is less than 2. For SSO and DSO fault cases, the value is between 2-10. Additionally, the proposed method detects the fault within one cycle of fault occurrence.

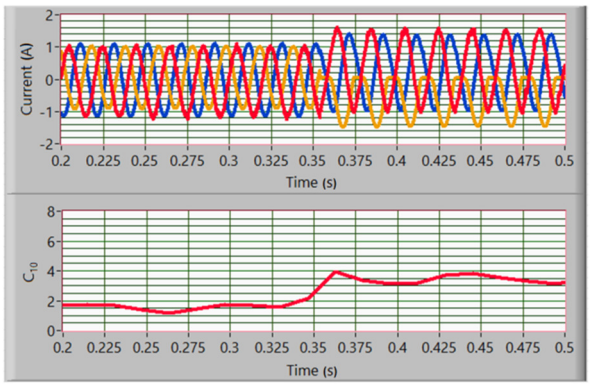

Fig. 16 Time-domain waveforms of stator currents and diagnostic signal (SSO fault)

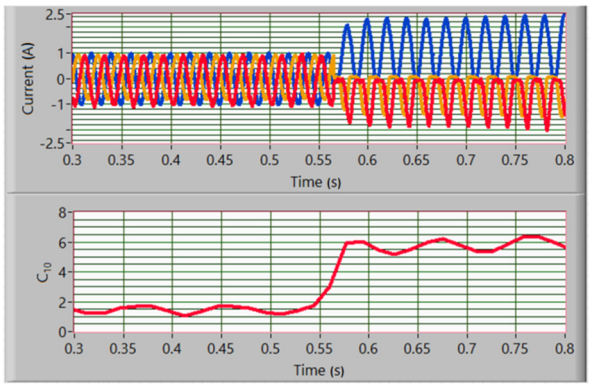

Fig. 17 Time-domain waveforms of stator currents and diagnostic signal (DSO fault)

7. Conclusions

The precise detection of a power switch failure in the inverter of IMDS is critical for its reliable operation. In this study, a novel index C_{10} is used for detecting SO and SS faults in the IMDS. An algorithm is also developed for localizing the fault in the inverter. The algorithm is capable of diagnosing and localizing the SO and SS faults in less than one cycle under any load and speed conditions. From the simulation results, the proposed index and the algorithm are seen to be capable of detecting, diagnosing, and localizing SO and SS faults. The experimental results also reiterate the effectiveness of the proposed algorithm in diagnosing SSO and DSO faults. Moreover, the algorithm can be easily implemented in FPGA, and hence it can provide an economical solution for fault diagnosis in industries. The proposed technique has potential application in SO and SS faults detection and localization in drive systems with multilevel inverter topologies. This technique can also be adapted for other types of faults in IMs and SO and SS faults in electric drives using PMSM and brushless DC motors.

Acknowledgment

The authors would like to thank Kerala State Council for Science, Technology, and Environment (KSCSTE) for the financial support for this study.

Conflicts of Interest

The authors declare no conflict of interest.

References

[1] O. Alshorman and A. Alshorman, "A Review of Intelligent Methods for Condition Monitoring and Fault Diagnosis of Stator and Rotor Faults of Induction Machines," International Journal of Electrical and Computer Engineering, vol. 11, no. 4, pp. 2820-2829, August 2021.

[2] X. Liang, M. Z. Ali, and H. Zhang, "Induction Motors Fault Diagnosis Using Finite Element Method: A Review," IEEE Transactions on Industry Applications, vol. 56, no. 2, pp. 1205-1217, March-April 2020.

[3] J. He, Q. Yang, and Z. Wang, "On-Line Fault Diagnosis and Fault-Tolerant Operation of Modular Multilevel Converters — A Comprehensive Review," CES Transactions on Electrical Machines and Systems, vol. 4, no. 4, pp. 360-372, December 2020.

[4] J. O. Estima, N. M. A. Freire, and A. J. M. Cardoso, "Recent Advances in Fault Diagnosis by Park's Vector Approach," IEEE Workshop on Electrical Machines Design, Control and Diagnosis (WEMDCD), pp. 279-288, March 2013.

[5] A. Hajary, R. Kianinezhad, S. G. Seifossadat, S. S. Mortazavi, and A. Saffarian, "Detection and Localization of Open-Phase Fault in Three-Phase Induction Motor Drives Using Second Order Rotational Park Transformation," IEEE Transactions on Power Electronics, vol. 34, no. 11, pp. 11241-11252, November 2019.

[6] S. Shi, Y. Sun, X. Li, H. Dan, and M. Su, "Moving Integration Filter-Based Open-Switch Fault-Diagnosis Method for Three-Phase Induction Motor Drive Systems," IEEE Transactions on Transportation Electrification, vol. 6, no. 3, pp. 1093-1103, September 2020.

[7] K. Hu, Z. Liu, I. A. Tasiu, and T. Chen, "Fault Diagnosis and Tolerance With Low Torque Ripple for Open-Switch Fault of IM Drives," IEEE Transactions on Transportation Electrification, vol. 7, no. 1, pp. 133-146, March 2021.

[8] W. Huang, L. Luo, J. Du, B. Xiang, S. Mei, L. Zhou, et al., "Open-Circuit Fault Detection in PMSM Drives Using Model Predictive Control and Cost Function Error," IEEE Transactions on Transportation Electrification, vol. 8, no. 2, pp. 2667-2675, June 2022.

[9] K. Hu, X. Meng, Z. Liu, J. Xu, G. Lin, and L. Tong, "Flux-Based Open-Switch Fault Diagnosis and Fault Tolerance for IM Drives with Predictive Torque/Flux Control," IEEE Transactions on Transportation Electrification. https://doi.org/10.1109/TTE.2022.3161988

[10] N. A. Mohar, E. Che Mid, S. M.Suboh, N. H.Baharudin, N. B. Ahamad, N. A. Rahman, et al., "Fault Detection Analysis for Three Phase Induction Motor Drive System Using Neural Network," Journal of Physics: Conference Series, vol. 1878, no. 1, article no. 012039, May 2021.

[11] M. Beibei, S. Yanxia, W. Dinghui, and Z. Zhipu, "Three Level Inverter Fault Diagnosis Using EMD and Support Vector Machine Approach," 12th IEEE Conference on Industrial Electronics and Applications (ICIEA), pp. 1595-1598, June 2017.

[12] B.Gmati, I.Jlassi, S. K. E.Khil, and A. J. M. Cardoso, "Open-Switch Fault Diagnosis in Voltage Source Inverters of PMSM Drives Using Predictive Current Errors and Fuzzy Logic Approach," IET Power Electronics, vol. 14, no. 6, pp. 1059-1072, May 2021.

[13] F. Asghar, M. Talha, and S. H. Kim, "Comparative Study of Three Fault Diagnostic Methods for Three Phase Inverter with Induction Motor," International Journal of Fuzzy Logic and Intelligent Systems, vol. 17, no. 4, pp. 245-256, December 2017.

[14] U. Abubakar, S.Mekhilef, K. S. Gaeid, H.Mokhlis, and Y. I. Al Mashhadany, "Induction Motor Fault Detection Based on Multi-Sensory Control and Wavelet Analysis," IET Electric Power Applications, vol. 14, no. 11, pp. 2051-2061, November 2020.

[15] M. A. Masrur, Z. Chen, and Y. Murphey, "Intelligent Diagnosis of Open and Short Circuit Faults in Electric Drive Inverters for Real-Time Applications," IET Power Electronics, vol. 3, no. 2, pp. 279-291, March 2010.

[16] N. S. Gameiro and A. J. Marques Cardoso, "A New Method for Power Converter Fault Diagnosis in SRM Drives," IEEE Transactions on Industry Applications, vol. 48, no. 2, pp.653-662, March-April 2012.
[17] J. F. Marques, J. O. Estima, N. S. Gameiro, and A. J. Marques Cardoso, "A New Diagnostic Technique for Real-Time Diagnosis of Power Converter Faults in Switched Reluctance Motor Drives," IEEE Transactions on Industry Applications, vol. 50, no. 3, pp. 1854-1860, May-June 2014.
[18] N. Mayadevi, V. P. Mini, R. H. Kumar, and S. Prins, "Fuzzy-Based Intelligent Algorithm for Diagnosis of Drive Faults in Induction Motor Drive System," Arabian Journal for Science and Engineering, vol. 45, no. 3, pp. 1385-1395, March 2020.
[19] M. Z. Ali, M. N. S. K. Shabbir, X. Liang, Y. Zhang, and T. Hu, "Machine Learning-Based Fault Diagnosis for Single- and Multi-Faults in Induction Motors Using Measured Stator Currents and Vibration Signals," IEEE Transactions on Industry Applications, vol. 55, no. 3, pp. 2378-2391, May-June 2019.
[20] S. M. K. Zaman and X. Liang, "An Effective Induction Motor Fault Diagnosis Approach Using Graph-Based Semi-Supervised Learning," IEEE Access, vol. 9, pp. 7471-7482, January 2021.
[21] S. Shao, R. Yan, Y. Lu, P. Wang, and R. X. Gao, "DCNN-Based Multi-Signal Induction Motor Fault Diagnosis," IEEE Transactions on Instrumentation and Measurement, vol. 69, no. 6, pp. 2658-2669, June 2020.
[22] A. R. Abbasi and M. R.Mahmoudi, "Application of Statistical Control Charts to Discriminate Transformer Winding Defects," Electric Power Systems Research, vol. 191, article no. 106890, February 2021.
[23] A. R. Abbasi, "Fault Detection and Diagnosis in Power Transformers: A Comprehensive Review and Classification of Publications and Methods," Electric Power Systems Research, vol. 209, article no. 107990, August 2022.
[24] V. P. Mini. N. Mayadevi, R. H. Kumar, and S. Ushakumari, "A Novel Algorithm for Detection and Diagnosis of Switching Faults of Three Phase Induction Motor Drive System," IEEE International Conference on Power Electronics, Drives and Energy Systems (PEDES), article no. 8707798, December 2018.
[25] Z. Yang, J. Liu, and H. Ouyang, "Open Fault Diagnose for SPWM Inverter Based on Wavelet Packet Decomposition," Lecture Notes in Electrical Engineering: Electronics and Signal Processing, vol. 97, no. 1, pp. 945-951, January 2011.
[26] M. Sifuzzaman, M. R. Islam, and M. Z. Ali, "Application of Wavelet Transform and Its Advantages Compared to Fourier Transform," Journal of Physical Sciences, vol. 13, pp. 121-134, 2009.
[27] J. A. Antonino-Daviu, M. Riera-Guasp, J. R. Folch, and M. P. M. Palomares, "Validation of a New Method for the Diagnosis of Rotor Bar Failures via Wavelet Transform in Industrial Induction Machines," IEEE Transactions on Industry Applications, vol. 42, no. 4, pp. 990-996, July-August 2006.
[28] F. Wu and J. Zhao, "Current Similarity Analysis-Based Open-Circuit Fault Diagnosis for Two-Level Three-Phase PWM Rectifier," IEEE Transactions on Power Electronics, vol. 32, no. 5, pp. 3935-3945, May 2017.
[29] W. S. Im, J. S. Kim, J. M. Kim, D. C. Lee, and K. B.Lee, "Diagnosis Methods for IGBT Open Switch Fault Applied to 3-Phase AC/DC PWM Converter," Journal of Power Electronics, vol. 12, no. 1, pp. 120-127, January 2012.
[30] W. S. Im, J. M. Kim, D. C. Lee, and K. B. Lee, "Diagnosis and Fault-Tolerant Control of Three-Phase AC–DC PWM Converter Systems," IEEE Transactions on Industry Applications, vol. 49, no. 4, pp. 1539-1547, July-August 2013.